nature physics

LETTERS

PUBLISHED ONLINE: 26 AUGUST 2012 | DOI: 10.1038/NPHYS2397

Strong-field physics with singular light beams

M. Zürch[1,2]*, C. Kern[1,2], P. Hansinger[1,2], A. Dreischuh[3] and Ch. Spielmann[1,2,4]*

Light beams carrying a point singularity with a screw-type phase distribution are associated with an optical vortex. The corresponding momentum flow leads to an orbital angular momentum of the photons[1–3]. The study of optical vortices has led to applications such as particle micro-manipulation[4,5], imaging[6], interferometry[7], quantum information[8] and high-resolution microscopy and lithography[9]. Recent analyses showed that transitions forbidden by selection rules seem to be allowed when using optical vortex beams[10]. To exploit these intriguing new applications, it is often necessary to shorten the wavelength by nonlinear frequency conversion. However, during the conversion the optical vortices tend to break up[11–13]. Here we show that optical vortices can be generated in the extreme ultraviolet (XUV) region using high-harmonic generation[14,15]. The singularity impressed on the fundamental beam survives the highly nonlinear process. Vortices in the XUV region have the same phase distribution as the driving field, which is in contradiction to previous findings[16], where multiplication of the momentum by the harmonic order is expected. This approach opens the way for several applications based on vortex beams in the XUV region.

Places where physical quantities become infinite or change abruptly are called singularities. The presence of phase dislocations (singularities) in the wavefront of a light beam determines both the phase and intensity structure around them. As the phase becomes indeterminate at singularities, both the real and the imaginary parts of the field amplitude (that is, also the field intensity) vanish. The characteristic helical phase profiles of optical vortices are described by $\exp(im\theta)$ multipliers, where θ is the azimuthal coordinate and the integer number m is their topological charge, also called dislocation strength or winding number.

Recalling the fact that in free space the Poynting vector gives the momentum flow, for helical phase fronts the Poynting vector has an azimuthal component that produces an orbital angular momentum parallel to the axis of the beam. The momentum circulates around the beam axis, so such beams are said to contain an optical vortex. As has been shown[1–3], an m-fold charged optical vortex beam carries an orbital angular momentum of $m\hbar$ per photon independent of the spin angular momentum (that is, the polarization state). It was shown that transitions that are forbidden by known selection rules in the electric and magnetic dipole approximation seem to be allowed when using optical vortex beams[10]. This provides a new degree of freedom in the spectroscopy of forbidden transitions. Multi-coloured optical vortices can be generated through a nonlinear frequency-conversion process such as second-harmonic generation[16] or four-wave mixing, which is an important process in the white-light vortex generation. However, as predicted in ref. 11 and observed in ref. 12, vortex break-up in self-focusing nonlinear media is an important issue for supercontinuum vortex generation[13].

On the other hand, the development of femtosecond lasers has paved the way towards time-resolved spectroscopy in the optical range. More recently the wavelength range of ultrashort pulses has been extended into the XUV region by nonlinear frequency conversion, termed as high-harmonic generation[17] (HHG). HHG is microscopically described by tunnel ionization, followed by propagation of the free electron in the laser field and finally recombination with the parent ion, accompanied by the emission of an XUV photon. The macroscopic build-up of the XUV radiation is governed by coherent superposition, and is limited by phase mismatch and re-absorption[15]. HHG-based XUV sources are nowadays widely used for spectroscopic applications owing to their ultrashort pulses in the attosecond range[18] and the high spatial and temporal coherence. Combining the unique properties of laser-driven XUV sources with the peculiarities of laser beams carrying orbital angular momentum will open new spectroscopic possibilities. Here we present the nonlinear frequency conversion of a near-infrared laser beam carrying a phase singularity into the XUV by HHG. It should be emphasized that, in contrast to previous wavelength conversion experiments relying on perturbative nonlinear optics, HHG is a non-perturbative nonlinear process[14,15,17,18].

The experiments are performed with a sub-30 fs laser system. With a reflective spatial light modulator (SLM) the helical phase is imprinted onto the laser beam, before focusing it into an argon target for HHG. The short-wavelength radiation is either analysed with a spectrometer or imaged onto a CCD (charge-coupled device) detector. All XUV images are taken after blocking the laser light with a thin Al filter. Further details are given in the Methods.

In a first step we studied whether the vortex structure is maintained during the highly nonlinear interaction of HHG. Without modulating the spatial phase of the laser beam, the XUV radiation is collinear with the laser beam and has a Gaussian intensity distribution (Fig. 1a). When imprinting a helical phase with the SLM in the centre of the Gaussian input mode, fragments of a doughnut-like structure with a vanishing intensity in the centre can be seen in the XUV region (see Fig. 1b). The two lobes are centred symmetrically around the XUV beam without phase modulation, and the signal in the centre vanishes within the dynamic range of the CCD (Fig. 1c). Applying a helical phase modulation, the XUV signal is about one order of magnitude lower when compared with a Gaussian fundamental mode. The lower integrated yield is explained by the strong intensity dependence[19] (roughly proportional to I^6) of the conversion efficiency. The missing parts of the XUV beam are attributed to a lack of phase matching[15,17] and the non-uniform intensity of the fundamental laser beam. Replacing the CCD with an imaging spectrometer, we checked whether the diameter of the doughnut depends on the harmonic order. As described in detail in the Supplementary Information, we found no significant dependence of the hole diameter on the harmonic order.

[1]Institute of Optics and Quantum Electronics, Friedrich-Schiller-University Jena, Max-Wien-Platz 1, 07743 Jena, Germany, [2]Abbe Center of Photonics, 07743 Jena, Germany, [3]Department of Quantum Electronics, Faculty of Physics, Sofia University, 5, J. Bourchier Blvd, BG-1164 Sofia, Bulgaria, [4]Helmholtzinstitut Jena, Fröbelstieg 3, 07743 Jena, Germany. *e-mail: michael.zuerch@uni-jena.de; christian.spielmann@uni-jena.de.

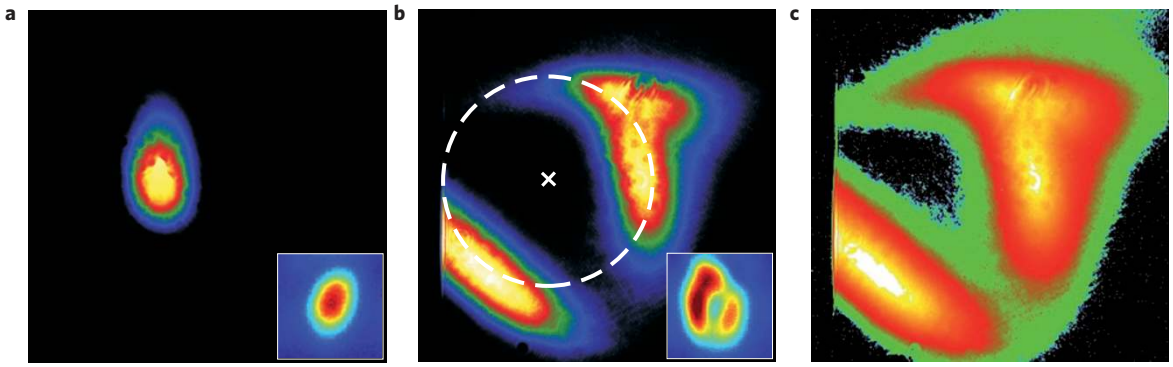

Figure 1 | Far-field intensity distributions of XUV light generated with Gaussian and vortex beams. a, Gaussian XUV beam produced by a Gaussian driving beam (insets show the corresponding infrared foci at the interaction region). **b**, An optical vortex in the XUV at 74 nm wavelength showing vanishing intensity in the centre (the cross coincides with the maximum of the Gaussian case (**a**) in the otherwise unchanged set-up) and fragments of a doughnut-like intensity distribution (dashed line to guide the eye) consisting of two lobes. A part of the beam on the left side is blocked with a razor blade to define the zero signal level. **c**, Same as **b** but with logarithmic intensity emphasising the zero intensity at the centre. Note the signal level in the centre is the same as in the shadow of the razor blade.

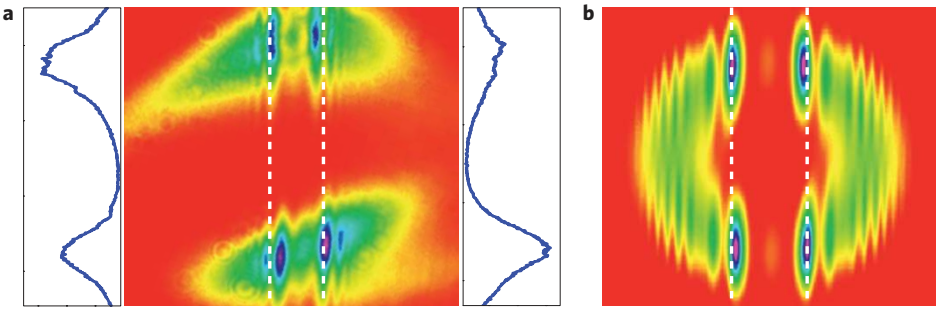

Figure 2 | Measurement and simulation of diffraction patterns of optical vortex beams caused by thin-wire diffraction. a, Measured fringe pattern of a vertical 5 μm tungsten wire. The shift of the fringes between the two lobes is clearly seen and also highlighted by the dashed lines and the corresponding line-outs. The vanishing intensity on the sides is caused by the lobe structure of the XUV beam. **b**, Results of a simulation predicting the thin-wire diffraction pattern of a beam carrying an optical vortex with a topological charge of 1. The shift of the fringes can be clearly seen. More details about the calculations are provided in the Supplementary Information.

The doughnut-like shape is a strong indication of an optical vortex; however, to strengthen the claim the helical phase has to be verified[20]. This is done by diffracting the XUV beam at a 5 μm tungsten wire behind the gas jet and recording the diffraction pattern (Fig. 2a). For these experiments we have not selected a single harmonic; however, the main contribution to the signal comes from the 23rd harmonic (36 nm wavelength) of the fundamental laser beam. In the recorded pattern in Fig. 2a the fringes in the two opposing lobes are shifted (dashed line in Fig. 2a), indicating a different phase in each of the two lobes. Simulations of thin-wire diffraction from beams (at 36 nm wavelength) carrying angular momentum (see Fig. 2b) reveal that an optical vortex with a topological charge of 1 reproduces the measured interference pattern best. More details are presented in Supplementary Section S5. As a final proof we measured the wavefront of the XUV beam[21] with a Hartmann sensor. Similar experiments in the optical range have shown that the wavefront should wind up like a screw around the singularity in the centre[22]. The measured XUV wavefront together with the intensity distribution is shown in Fig. 3. It can be clearly seen that two lobes of the XUV beam with non-vanishing signal have an opposite tilt of the wavefront. These two observations back our claim of an optical vortex in the XUV with a topological charge of 1.

From the theory of HHG (ref. 23), an N-times multiplied phase for the Nth harmonic is expected and thus the topological charge of the harmonic should be the fundamental topological charge times N, accordingly. Moreover, this phase relationship holds true for any periodic process, where the radiating dipole is a function of the phase of the driving field $d(t) = f(\exp(i[\omega t + \varphi]))$. The Nth harmonic of this field is given by the Fourier transform $\tilde{d}(N\omega) = \int \exp(iN\omega)d(t)\,\mathrm{d}t$, which immediately yields the phase relationship $\varphi(N\omega) = N\varphi(\omega)$. However, the fact that the diameter of the XUV beam is independent of harmonic order, together with the interferometric measurements summarized in Fig. 2 and the measured wavefront, provides clear evidence of an optical vortex with a topological charge of 1, for all harmonic orders. The unintuitive experimental observation of topological charge of 1 is explained as follows: initially, the Nth harmonic carries an N-times charged optical vortex. The strong background beam modulation and the strong perturbations in the HHG process force the optical vortex to decay into single-charged optical vortices. The decay is enhanced by the fact that all topological charges carry the same sign, so they will strongly repel each other (eventually also rotating during propagation)[24]. Most of the high-order optical vortices escape from the central part of the beam, thus remaining invisible outside the oscillating wings of the field behind the wire, as shown in Fig. 2b. Deviations of the driving laser field from a perfect Gaussian beam result in a non-ideal intensity distribution in the focus (Fig. 1b inset). An extended discussion is provided in Supplementary Section S4.

We also ventured to verify that XUV radiation can be generated with a fundamental beam carrying a topological charge greater

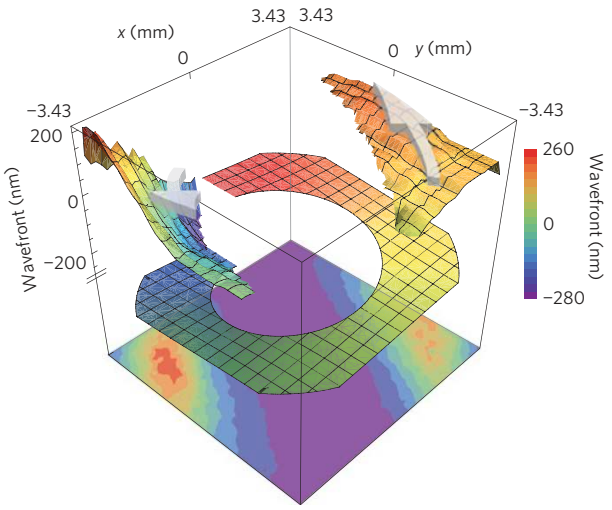

Figure 3 | Wavefront measurement of an optical vortex beam. Wavefront of an optical vortex evaluated at points where the signal intensity is above $1/e^2$ of the maximum in the XUV region reconstructed from a Hartmann measurement (upper layer). The wavefront is tilted in opposite directions for opposing lobes of the XUV vortex beam, and a screw-type evolution is seen (indicated by two white arrows to guide the eye). The intermediate layer shows the theoretically expected shape, also only for points where, in a complete vortex ring, the signal intensity would be measured. The scales represent the actual size of the beam at the Hartmann mask. The colour scale corresponds to the intermediate and upper layers. The bottom layer shows the intensity distribution at the Hartmann mask, showing that owing to limited size only a part of the lobes would be measured. The signal amplitude (arbitrary scale) is lowest for purple and maximum for red. In the purple area the signal level is too low for an evaluation of the phase front.

than 1. For an input beam with a topological charge of 2, we observed a similar intensity distribution consisting of two lobes, but with increased distance from the centre. This observation suggests a higher topological charge for the XUV beam, as shown in detail in the Supplementary Information. However, for input beams carrying a topological charge of 2 or higher, the XUV beam was too weak for a detailed analysis.

We have shown the possibility of transferring angular momentum of an ultrashort pulse laser beam from the infrared spectral domain into the XUV using the highly nonlinear effect of HHG. From the measurements done in both the spatial and spectral (see Supplementary Information) domain, evidence for the generation of an optical vortex beam in the XUV at around 36 nm wavelength is provided. The most remarkable observation is that the singularity can survive the highly nonlinear process of HHG, even though strong ionization takes place[25]. Apart from the already known possibility of second-harmonic generation and four-wave mixing[26,27], another field of nonlinear interaction with beams having an angular momentum is added by this research. The observed structure is not a perfect optical vortex yet, owing to azimuthal instabilities and decay taking place in the generation process. However, the resulting double-lobe structure clearly shows the main features of a singularity in the centre and the phase evolution around this singularity. The measured topological charge of 1 and the observed scaling is in contradiction to theoretical predictions. Taking the decay of the highly charged optical vortex into account, the results can be well explained. However, some details still remain unclear and must be further studied to fully understand the generation process. Laser beams with singularities offer already many applications in the optical domain. The research presented here paves the way to extend the wavelength range into the XUV region. Possible applications rely on the ultrashort nature of the XUV radiation, opening the possibility of steering and controlling electrons with beams having angular momentum on the attosecond timescale.

Methods

The set-up is shown in detail in Supplementary Fig. S2. A femtosecond laser system producing pulses with sub-30 fs pulse duration at 800 nm wavelength and energies up to 1 mJ at a repetition rate of 1 kHz was used. Using a reflective-type SLM, a calculated phase profile is transferred from a computer to the SLM, and arbitrary phase patterns can be embedded in the fundamental laser beam[28]. These modified laser pulses are then focused ($f = 300$ mm, $f/\# = 15$) into the interaction region to a diameter of roughly 40 μm, resulting in peak intensities of approximately 2×10^{15} W cm^{-2} (ref. 29). The interaction region consists of a nickel tube (2 mm diameter) sealed at the end and squeezed ($d \sim 1$ mm) to a flat surface facing the laser beam. The laser itself drills a hole in the tube, large enough so that both Gaussian and vortex beams can fit into the interaction region to where the argon is supplied. A long-distance microscope is used to monitor the laser focus. Typical phase masks and technical details are given in Supplementary Section S2.

For the phase measurement presented in Fig. 2, the wavefront splitting technique by introducing a thin wire into the beam was used[20]. A 5-μm-thick tungsten wire was placed at a distance of 8 cm downstream of the HHG source. The fringe spacing revealed that the wavelength was around 36 nm.

The Hartmann set-up to acquire the wavefront (Fig. 3) is described elsewhere[29]. The Hartmann pattern obtained from illumination of the mask with a Gaussian fundamental mode was used for calibration to remove intrinsic aberrations present in the XUV beam. To do so, the pattern of the Gaussian mode was assumed as a reference. The recorded Hartmann pattern of the optical vortex thus represents a differential wavefront in comparison with a Gaussian beam of otherwise identical experimental conditions.

Received 12 January 2012; accepted 17 July 2012; published online 26 August 2012

References

1. Allen, L., Barnett, S. M. & Padget, M. J. *Optical Angular Momentum* (Institute of Physics, 2004).
2. Tabosa, J. W. R. & Petrov, D. V. Optical pumping of orbital angular momentum of light in cold cesium atoms. *Phys. Rev. Lett.* **83,** 4967–4970 (1999).
3. Barreiro, S. & Tabosa, W. R. Generation of light carrying orbital angular momentum via induced coherence grating in cold atoms. *Phys. Rev. Lett.* **90,** 133001 (2003).
4. Grier, D. G. *et al.* A revolution in optical manipulation. *Nature* **424,** 810–816 (2003).
5. Padgett, M. & Bowman, R. Tweezers with a twist. *Nature Photon.* **5,** 343–348 (2011).
6. Foo, G., Palacios, D. M. & Swartzlander, G. A. Jr Optical vortex coronagraph. *Opt. Lett.* **30,** 3308–3310 (2005).
7. Furhapter, S., Jesacher, A., Bernet, S. & Ritsch Marte, M. Spiral interferometry. *Opt. Lett.* **30,** 1953–1955 (2005).
8. Molina Terriza, G., Torres, J. P. & Torner, L. Twisted photons. *Nature Phys.* **3,** 305–310 (2007).
9. Scott, T. F., Kowalski, B. A., Sullivan, A. C., Bowman, C. N. & McLeod, R. R. Two-color single-photon photoinitiation and photoinhibition for subdiffraction photolithography. *Science* **324,** 913–917 (2009).
10. Picón, A. *et al.* Transferring orbital and spin angular momenta of light to atoms. *New J. Phys.* **12,** 083053 (2010).
11. Firth, W. J. & Skryabin, D. V. Optical solitons carrying orbital angular momentum. *Phys. Rev. Lett.* **79,** 2450–2453 (1997).
12. Tikhonenko, V., Christou, J. & Luther-Daves, B. Spiraling bright spatial solitons formed by the breakup of an optical vortex in a saturable self-focusing medium. *J. Opt. Soc. Am. B* **12,** 2046–2052 (1995).
13. Neshev, D. N., Dreischuh, A., Maleshkov, G., Samoc, M. & Kivshar, Y. S. Supercontinuum generation with optical vortices. *Opt. Express* **18,** 18368–18373 (2010).
14. L'Huillier, A. & Balcou, P. High-order harmonic generation in rare gases with a 1-ps 1053-nm laser. *Phys. Rev. Lett.* **70,** 774–777 (1993).
15. Brabec, T. & Krausz, F. Intense few-cycle laser fields: Frontiers of nonlinear optics. *Rev. Mod. Phys.* **72,** 545–591 (2000).
16. Toda, Y., Honda, S. & Morita, R. Dynamics of a paired optical vortex generated by second-harmonic generation. *Opt. Express* **18,** 17796–17804 (2010).
17. Winterfeldt, C., Spielmann, C. & Gerber, G. Colloquium: Optimal control of high-harmonic generation. *Rev. Mod. Phys.* **80,** 117–140 (2008).
18. Krausz, F. & Ivanov, M. Attosecond physics. *Rev. Mod. Phys.* **81,** 163–234 (2009).
19. Constant, E. *et al.* Optimizing high harmonic generation in absorbing gases: Model and experiment. *Phys. Rev. Lett.* **82,** 1668–1671 (1999).
20. Peele, A. & Nugent, K. X-ray vortex beams: A theoretical analysis. *Opt. Express* **11,** 2315–2322 (2003).
21. Starikov, F. A. *et al.* Wavefront reconstruction of an optical vortex by a Hartmann–Shack sensor. *Opt. Lett.* **32,** 2291–2293 (2007).

22. Murphy, K., Burke, D., Devaney, N. & Dainty, C. Experimental detection of optical vortices with a Shack–Hartmann wavefront sensor. *Opt. Express* **18,** 15448–15460 (2010).
23. Lewenstein, M., Balcou, P., Ivanov, M. Y., L'Huillier, A. & Corkum, P. B. Theory of high-harmonic generation by low-frequency laser fields. *Phys. Rev. A* **49,** 2117–2132 (1994).
24. Indebetouw, G. Optical vortices and their propagation. *J. Mod. Opt.* **40,** 73–87 (1993).
25. Vincotte, A. & Berge, L. Femtosecond optical vortices in air. *Phys. Rev. Lett.* **95,** 193901 (2005).
26. Basistiy, I. V., Bazhenov, V. Y., Soskin, M. S. & Vasnetsov, M. V. Optics of light beams with screw dislocations. *Opt. Commun.* **103,** 422–428 (1993).
27. Zhang, Y. *et al.* Modulated vortex solitons of four-wave mixing. *Opt. Express* **18,** 10963–10972 (2010).
28. Neil, M. A. A., Booth, M. J. & Wilson, T. Dynamic wavefront generation for the characterization and testing of optical systems. *Opt. Lett.* **23,** 1849–1851 (1998).
29. Lohbreier, J. *et al.* Maximizing the brilliance of high-order harmonics in a gas-jet. *New J. Phys.* **11,** 023016 (2009).

Acknowledgements

M.Z. acknowledges support from the FSU grant ProChance 2009 A1. C.K. acknowledges support from a fellowship of the Abbe School of Photonics Jena. A.D. acknowledges support from FSU-IOQ and from NSF (Bulgaria) under contract DRNF-02/8/2009.

Author contributions

C.S. and A.D. initiated the project. M.Z. and C.K. performed the experiments. M.Z., C.K. and P.H. analysed the data. A.D. supplied theoretical background and set up a simple model for explanation of the effects. All authors have participated in the interpretation of the experiments and contributed to the manuscript.

Additional information

Supplementary information is available in the online version of the paper. Reprints and permissions information is available online at www.nature.com/reprints. Correspondence and requests for materials should be addressed to M.Z. or C.S.

Competing financial interests

The authors declare no competing financial interests.